

## EVEN-PARITY BANDS OF $^{108,110,112}\text{Ru}$

S. J. ZHU<sup>\*,†,‡,‡‡</sup>, Y. X. LUO<sup>†,§</sup>, J. H. HAMILTON<sup>†</sup>, A. V. RAMAYYA<sup>†</sup>,  
X. L. CHE<sup>\*</sup>, Z. JIANG<sup>\*</sup>, J. K. HWANG<sup>†</sup>, J. L. WOOD<sup>¶</sup>, M. A. STOYER<sup>||</sup>,  
R. DONANGELO<sup>\*\*</sup>, J. D. COLE<sup>††</sup>, C. GOODIN<sup>†</sup> and J. O. RASMUSSEN<sup>§</sup>

<sup>\*</sup>Physics Department, Tsinghua University, Beijing 100084, China

<sup>†</sup>Physics Department, Vanderbilt University, Nashville, TN 37235, USA

<sup>‡</sup>Joint Institute for Heavy Ion Research,

Oak Ridge National Lab, Oak Ridge, TN 37830, USA

<sup>§</sup>Lawrence Berkeley National Laboratory, Berkeley, CA 94720, USA

<sup>¶</sup>School of Physics, Georgia Institute of Technology, Atlanta, GA 30332, USA

<sup>||</sup>Lawrence Livermore National Laboratory, Livermore, CA 94550, USA

<sup>\*\*</sup>Universidade Federal do Rio de Janeiro, CP 68528, RJ Brazil

<sup>††</sup>Idaho National Laboratory, Idaho Falls, ID 83415, USA

<sup>‡‡</sup>zhushj@mail.tsinghua.edu.cn

Accepted 2 April 2009

High-spin, even-parity bands in neutron-rich  $^{108,110,112}\text{Ru}$  nuclei were reinvestigated and considerably expanded by measuring many-fold prompt  $\gamma$ -ray coincidence events following the spontaneous fission of  $^{252}\text{Cf}$  with Gammasphere. Our high statistics data allow us to detect weaker transitions and bands not previously published. Also, gamma branching ratios, which are important for theory, are carefully measured from all levels. In  $^{110}\text{Ru}$ , we find a doubling of levels for both ground and quasi-gamma bands above the  $8^+$  levels. There are likely two-phonon quasi-gamma bands in  $^{110,112}\text{Ru}$ , as well as a bandhead level in  $^{108}\text{Ru}$ . The odd–even spin energy band staggering observed in the quasi-gamma bands in  $^{108,110,112}\text{Ru}$  and the doubling of levels in  $^{110}\text{Ru}$  present a challenge to theory.

*Keywords:* Even-parity bands; triaxial deformation; band crossing; quasi-gamma bands.

PACS Number(s): 21.10.Re, 25.85.Ca, 27.60.+j

### 1. Introduction

The neutron-rich  $^{108,110,112}\text{Ru}$  nuclei lie within the  $A \sim 100$  deformed region. It is difficult to study the high-spin states of these nuclei using normal heavy-ion nuclear reactions. One powerful method is to measure coincidence events among the prompt  $\gamma$ -rays from spontaneous fission of heavy nuclei, such as  $^{252}\text{Cf}$ .<sup>1</sup> In the earlier beta-decay studies of Äystö *et al.*,<sup>2</sup> the systematics of the lower-spin members of the ground bands were published for  $^{108,110,112}\text{Ru}$ . They also presented theoretical calculations of Hartree–Fock (HF) energy surfaces, suggesting that the minimum nuclear shape starts near prolate spheroidal, but migrates toward triaxial as one

goes from mass 108 to 110 to 112 in Ru. In previous publications, studying prompt gamma rays from the spontaneous fission of  $^{248}\text{Cm}$  or  $^{252}\text{Cf}$ , some collective band structures of  $^{108,110,112}\text{Ru}$  were reported<sup>3-7</sup> and triaxial deformation was proposed. Already in 1994, Shannon *et al.*<sup>3</sup> established ground band levels up to  $10^+$  for  $^{108,110,112,114}\text{Ru}$ . In the early publication of Lu *et al.*,<sup>4</sup> the spins of the ground bands of  $^{108,110,112}\text{Ru}$  were extended up to  $16^+$ , and band-crossing above spins  $10^+$  and  $12^+$  for  $^{108}\text{Ru}$  and  $^{110}\text{Ru}$  were observed, respectively. No band-crossing, but a smooth crossing, was found in  $^{112}\text{Ru}$  above  $10^+$ . The subsequent work of Lu *et al.*<sup>4</sup> extended the one-phonon quasi-gamma bands and provided first evidence of the two-phonon quasi-gamma bands in the Ru isotopes.

Deloncle *et al.*<sup>5</sup> from heavy-ion reaction work at the Eurogam array published the level-scheme systematics of  $^{108}\text{Ru}$  and lighter isotopes, along with supporting theoretical work. The 2003 Gammasphere work by Hua *et al.*<sup>6</sup> with alpha-induced-fission of uranium and Doppler correction for fission gammas emitted in flight followed the ground band of Ru and Pd nuclei up through the band-crossings and convincingly associated the crossings with alignment of an  $h_{11/2}$  neutron pair. In a later publication from the same experiment and collaboration, Wu *et al.*<sup>7</sup> show the ground bands up to  $22^+$  for  $^{110}\text{Ru}$  and  $^{112}\text{Ru}$ . They associate also the first band-crossing in these two nuclei with alignment of a pair of  $h_{11/2}$  neutrons. They show evidence of a second band-crossing, attributed to alignment of a pair of  $g_{9/2}$  protons slightly higher in  $^{112}\text{Ru}$ , and this assignment is supported by a similar band-crossing in  $^{111}\text{Ru}$ , where the neutron pairing would be blocked. Recently, Möller *et al.* performed global calculations of ground-state nuclear energies with axial shape asymmetry and found that  $^{108}\text{Ru}$  has the most stabilization for triaxial shape.<sup>8</sup>

In the present paper, we show and discuss the even-parity bands of neutron-rich  $^{108,110,112}\text{Ru}$  nuclei updated in the present work. The ground bands and one-phonon quasi-gamma bands were carefully remeasured with our high statistics data. Due to Doppler-smearing of transitions from the few picosecond (shorter lifetimes than fission fragment slowing-down times in iron backing and cover), we usually could not observe the highest-spin levels of the ground band reported in Refs. 6 and 7. However, our higher statistics data from stopped fragments enabled us to identify weak bands and branching transitions in these bands, not reported before. Bands with  $(4^+)$  bandhead and energies between two and three times the energy of the second  $2^+$  bandheads are found in  $^{110,112}\text{Ru}$ , which we assign as a collective band associated with two-phonon quasi-gamma excitation. A two-phonon quasi-gamma bandhead  $(4^+)$  is assigned to  $^{108}\text{Ru}$ . The  $(4^+)$  assignment is on the basis of a 466.6 keV transition from a  $(5^-)$  level, the spin of which is proven by angular correlation. (See text in Sec. 2 and the legend of Fig. 6 in our companion paper on Odd-parity bands of  $^{108,110,112}\text{Ru}$ .) We use the more general term “quasi-gamma band” of Sakai,<sup>9</sup> rather than “gamma-vibrational band” or “triaxial-rotor sideband” of Davydov and Filippov.<sup>10</sup> As is well known, the  $2^+$  sidebands in regions of triaxial softness or deformation do not have a good projection quantum number  $K = 2$ ,

since there is generally extensive  $K$ -mixing.) A weakly populated doubling of levels to both ground and quasi-gamma bands is observed in  $^{110}\text{Ru}$ . The odd-even spin energy staggering are observed and discussed in  $^{110,112}\text{Ru}$ . An excited  $0^+$  band is confirmed and extended in  $^{108}\text{Ru}$ .

Frauendorf and others have developed a theory of chiral doubling in rotational bands of triaxial nuclei.<sup>11,12</sup> A number of cases have been proposed from experimental level schemes, mostly in odd-odd nuclei with neutron numbers somewhat below 82.<sup>13,14</sup> The theoretical model of nuclear chirality requires nuclei of triaxial shape and at least one particle-like nucleon and one hole-like nucleon, preferably from the higher- $j$  orbitals near the Fermi energy. The angular-momentum vector of the particle-like nucleon will have its energetically most favorable orientation tending along the shortest principal axis of the nuclear ellipsoid. Likewise, the hole-like nucleon will prefer to orient along the longest axis. The collective rotation preferentially aligns along the nuclear axis of intermediate length, since the core rotational moment-of-inertia (hydrodynamic or cranking) will be largest along the nuclear axis of intermediate length. This is the case because the eccentricity of the equatorial planar ellipse is largest for the axis of intermediate length. The chirality manifests itself as a doubling of rotational bands, each spin-parity combination occurring twice. Each chiral band is an equal linear combination of the left-handed and right-handed forms for the three mutually perpendicular angular-momentum vectors. The linear combination has a complex phase factor which may vary with spin.

We have reported on the level schemes and proposed soft chiral vibrations in odd-parity bands of  $^{106}\text{Mo}$ .<sup>15,16</sup> In a recent conference paper, we proposed the likely chiral doublet nature of odd-parity bands in  $^{110,112}\text{Ru}$  nuclei.<sup>17</sup> A band in  $^{110}\text{Ru}$  with bandhead at 3193.3 keV and apparent E2 cascade of four transitions down from a level at 6017.4 keV was reported by our collaboration in Jiang *et al.*<sup>18,19</sup> This doubling of the ground band in  $^{110}\text{Ru}$  is observed above the  $8^+$  level, and the branches are close in energy. In the present work, we observed a new doubling of the even-spin members of the one-phonon quasi-gamma band above spin 8 in  $^{110}\text{Ru}$ .

This paper will concentrate on presenting the experimental data and comparing with earlier work. Our some time collaborators on theoretical aspects, Stefanescu, Gelberg, and others<sup>20</sup> used energies and gamma branching ratios in the tables of a draft of the present paper. They used the IBM-1 model (Interacting Boson Model) to fit these data. New Total Routhian Surface (TRS) calculations were performed for the present paper to investigate the nuclear shape at zero and at higher spin. Though there are several previous publications of energy surfaces in this region of triaxiality, we felt it useful to make the TRS calculations to learn more about the sensitivity of the results to input parameters. Routhians for  $^{108,110,112}\text{Ru}$  are also calculated using cranked shell-model (CSM) to interpret the band-crossings.

## 2. Experiment and Results

Our experiment was carried out at the Lawrence Berkeley National Laboratory in 2000. The  $^{252}\text{Cf}$  source of strength  $\sim 60 \mu\text{Ci}$  was sandwiched between two iron foils with a thickness of  $10 \text{ mg/cm}^2$  and placed at the center of the Gammasphere detector array which, for this experiment, consisted of 101 Compton-suppressed Ge detectors. A total of  $5.7 \times 10^{11}$  triple- and higher-fold coincidence events were collected. The coincidence data were analyzed with the standard Radware software package,<sup>21</sup> and later by a new ‘‘Radware cube’’ (three-dimensional gamma-energy histogram) program with less channel compression. We have projected hundreds of double-gated gamma spectra in building level schemes up from the low-spin levels known from earlier published work in the nuclear databases. Furthermore, we cross-check with gating on fission partner Xe transitions. Figures 1(a) and (b) are two examples of the  $^{110}\text{Ru}$  gated spectra, illustrating the quality of the high-statistics spectral data as displayed by the less-compressed version of Radware.

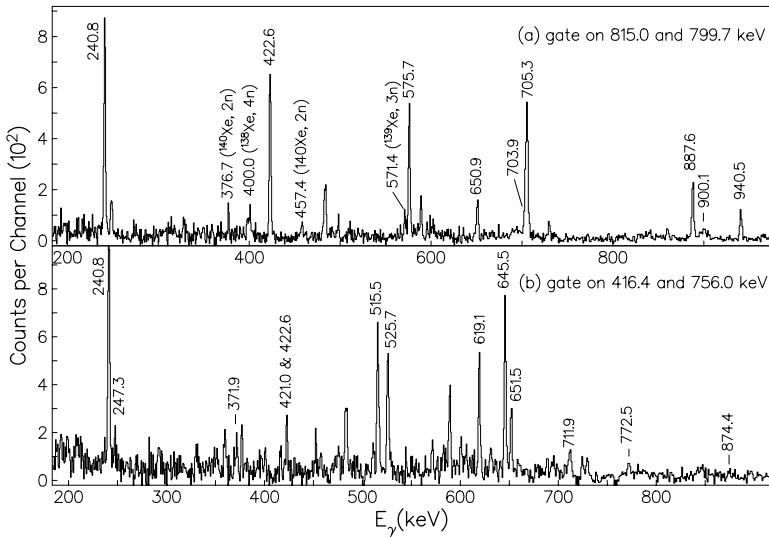


Fig. 1. Examples of double-gated gamma spectra showing a new band and new levels in  $^{110}\text{Ru}$ . In spectrum 1(a), the gates are set on the  $10 \rightarrow 8$  and the  $16 \rightarrow 14$  transitions of the ground band (1). (See Fig. 3, the  $^{110}\text{Ru}$  even-parity level scheme.) This gated spectrum shows the newly observed 650.9–940.5 keV cascade and all the rest of the sequence of ground-band transitions assigned by Wu *et al.*<sup>7</sup> up to the  $18^+$  level. Note that the 900.1 keV  $18 \rightarrow 16$  transition shows Doppler broadening in our spectrum, since the fission fragment slowing-down time in the iron foil sandwich is comparable to the few picosecond lifetime of the  $18^+$  state. The two higher transitions of 1003 keV and 1106 keV reported in Ref. 7 are off-scale in Fig. 1 but are not observable by us, presumably because of the Doppler broadening. In spectrum 1(b), the first gate is set on a 416.4 keV decay-out transition from new band (8) (see Fig. 3) to the  $9^+$  member of the quasi-gamma band (2) and the second gate on the 756.0 keV  $9 \rightarrow 7$  transition in band (2).

Figure 1(a) shows gating in the ground band (1) above and below a weaker parallel path not hitherto published. Gates are set on the  $10 \rightarrow 8$  transition of 815.0 keV and the  $16 \rightarrow 14$  transition of 799.7 keV. The projected spectrum shows not only the previously known stronger cascade of 887.6 keV and the shoulder 703.9 keV (almost masked by the intense lower  $8 \rightarrow 6$  transition of 705.3 keV), but also a weaker new 650.9–940.5 keV cascade, through what can only be another  $12^+$  level at 3700.1 keV. The new 3700.1 keV level is further confirmed in cross-checking, especially in the double-gated spectrum (not shown) by a 670.4 keV transition from the  $14^+$  level of a new band (8).

Figure 1(b) shows a double-gated spectrum revealing the existence of new band (8). The gates are set on the strong 416.4 keV transition going to the  $9^+$  level of the quasi-gamma band (2). The other gate is set at 756.0 keV, the transition from the  $9^+ \rightarrow 7^+$  level of band (2). The projected spectrum (Fig. 1(b)) clearly shows the transitions going up new band (8): 525.7, 651.5, and 772.5 keV. The highest transition of band (8) is barely seen in this spectrum but confirmed by other gating combinations.

Our even-parity level schemes in  $^{108,110,112}\text{Ru}$  are shown in Figs. 2–4. Although Doppler smearing from few picosecond lifetime levels prevent our observing the highest-spin level of the ground bands reported by Wu *et al.*,<sup>7</sup> our high statistics data allow us to considerably expand the level schemes with identifications of a series of weak transitions and bands (see captions of Figs. 2–4). We will concentrate only on even-parity levels populated by spontaneous fission (together with some even-parity levels populated by the same fissioning source via  $^{108,110}\text{Tc}$  beta decay.) The odd-parity level schemes populated by spontaneous fission are given in the companion paper to this one.<sup>22</sup> This split into two papers is facilitated by the fact that the weakly populated odd-parity bands decay-out into the even-parity bands without known transitions from even-parity to odd-parity.

It is worth emphasizing that the considerably extended one-phonon quasi-gamma band (2) with two signature partners reaches as high as  $17^+$ ,  $13^+$ , and  $13^+$  for  $^{112}\text{Ru}$ ,  $^{110}\text{Ru}$ , and  $^{108}\text{Ru}$ , respectively, with excitation energies a bit lower than but comparable to those of the ground bands (see Figs. 2–4). In Ref. 7, they state that the energies of transitions in their quasi-gamma band may be uncertain by 1 keV, an order of magnitude greater than ours. Thus, our level energies differ from Ref. 7 by as much as 2 keV in some cases.

The two-phonon quasi-gamma bands (band 3) identified in this work are also shown in Figs. 2–4. In a preliminary analysis by our collaboration,<sup>23</sup> we proposed bandheads of the two-phonon quasi-gamma band in all three nuclei. Stachel *et al.*<sup>24</sup> carried out  $\gamma$ - $\gamma$  directional correlation measurements in the course of their work on  $^{108}\text{Ru}$  and assigned the spin/parity of the 1825.9 keV level as  $2^+$ . We accept their assignment and retract the  $5^+$  value. Stachel *et al.*<sup>24</sup> assigned a mixed dipole–quadrupole transition from the 1825.9 keV level to the  $2^+$  first-excited state, which requires even-parity. The beta-decay work<sup>24</sup> did not assign a spin to the weakly

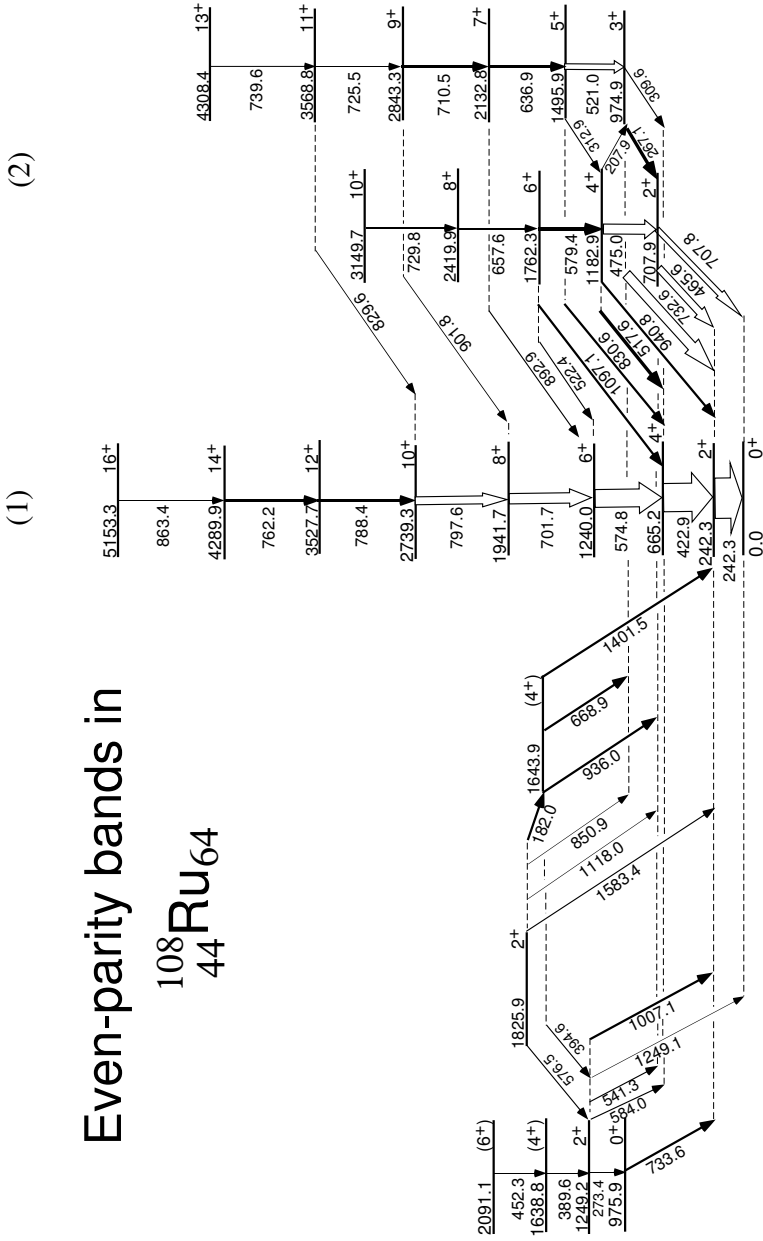


Fig. 2. The level scheme for even-parity bands in  $^{108}\text{Ru}$ . Here, we include as un-numbered levels to the left of ground band (1) several low-spin levels studied first in the beta-decay of  $^{108}\text{Tc}$ . We observe them because this beta-decay feeds levels decaying by triple gamma cascades. We have not attempted to determine the proportion due to beta decay from that due to prompt fission gammas. Prompt fission is feeding the excited  $0^+$  band, since we find  $4^+$  and  $6^+$  members, not observed in beta-decay studies. The ( $4^+$ ) level at 1643.9 keV is assigned as the bandhead of the two-phonon quasi-gamma band in  $^{108}\text{Ru}$  (see text).

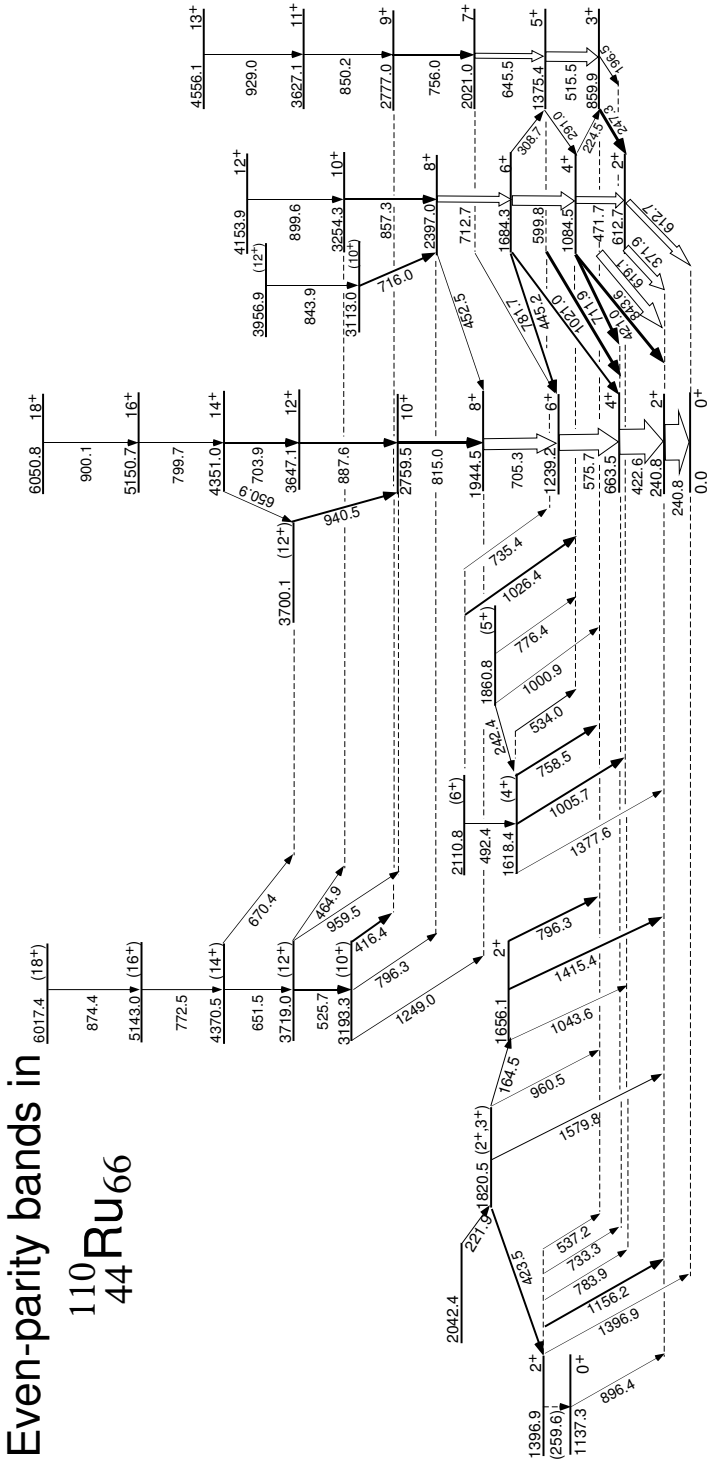


Fig. 3. The considerably expanded level scheme for even-parity bands in <sup>110</sup>Ru. Note the sequence of new-band (8) transitions of 525.7, 651.5, 772.5, and 874.4 keV. The spin-parity sequence of band (8) could have odd-parity and odd spins one unit less than the assignments shown, an uncertainty that may perhaps be resolved by angular correlation work on decay-out transitions. Note also the doubling of the quasi-gamma band (2) above the 8<sup>+</sup> state, a feature not previously reported. Our level scheme shows the four lowest  $\Delta I = -1$  cascade transitions between signature partners, where none were shown in Ref. 7. The assignment of band (3) as a two-phonon quasi-gamma band is supported by the fact that it decays-out mainly to the one-phonon quasi-gamma band (see Sec. 3).

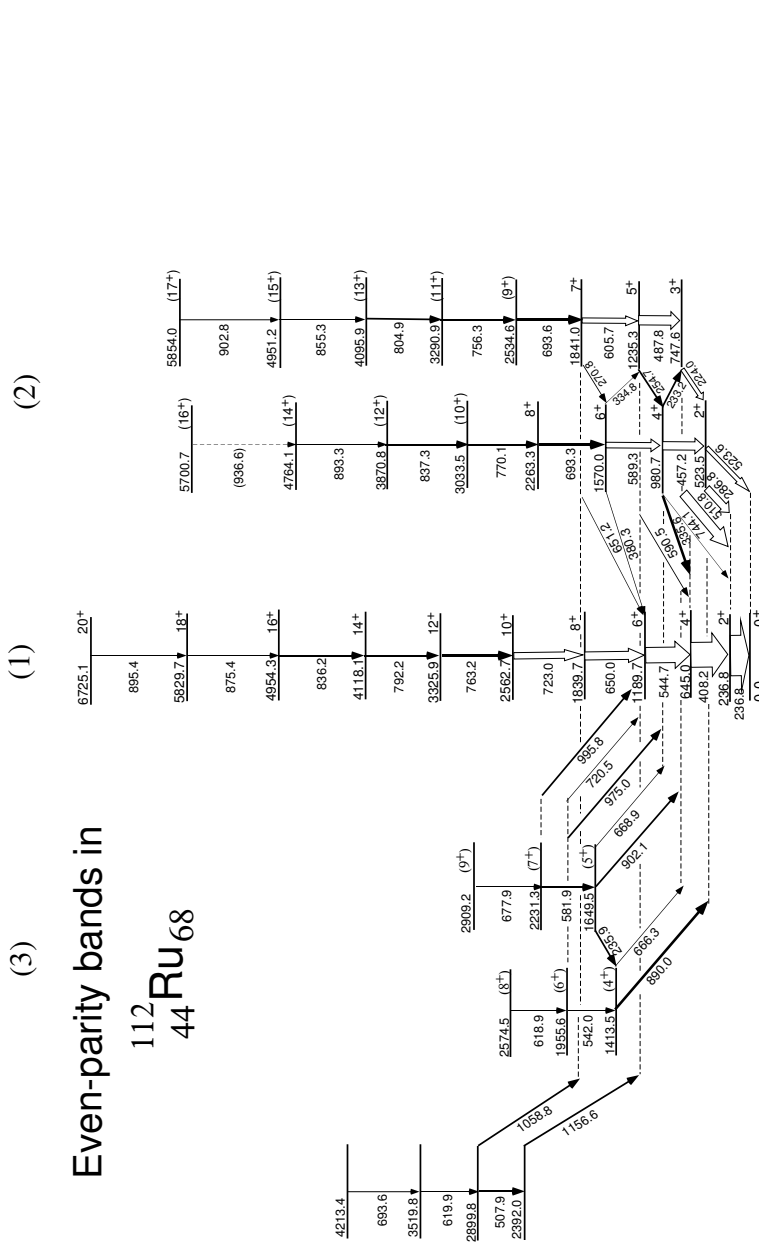


Fig. 4. The considerably expanded level scheme for even-parity bands in  $^{112}\text{Ru}$ . Note the stronger evidence that band (3) with six identified members is a higher quasi-gamma band. Its decay-out transitions go predominantly to the first quasi-gamma band (see details in Sec. 3). The comparison with Fig. 7 level scheme of Wu *et al.*<sup>7</sup> shows that they go to one higher level in the ground band. However, our scheme goes one spin higher in the even-spin signature quasi-gamma band; we differ in the  $14 \rightarrow 12$  transition, they selecting a 918.0 keV transition and we selecting an 893.3 keV transition, with a tentative assignment for a  $16 \rightarrow 14$  transition of 936.6 keV. Their level scheme shows five transitions from the quasi-gamma band, and ours shows eight. Their scheme shows one  $\Delta J = -1$  transition in the quasi-gamma band, and ours shows five.

populated 1643.9 keV level in  $^{108}\text{Ru}$ . In studying the odd-parity bands, as reported in the accompanying article of Luo *et al.*,<sup>22</sup> we found a transition to the 1643.9 keV level from a  $5^-$  level, where the spin was proved by angular correlation. This established the  $4^+$  assignment. The energy of this level is close to what is expected from the systematics of two-phonon quasi-gamma bandheads in  $^{110,112}\text{Ru}$ . Thus, we think this  $4^+$  level is the two-phonon quasi-gamma bandhead. This assignment is supported by the fact that the strongest depopulation of the 1643.9 keV level is to the one-phonon quasi-gamma band members, not ground band, just as with the two-phonon quasi-gamma bandheads in  $^{110,112}\text{Ru}$ . (More details are given in Sec. 3.)

Regarding the quasi-gamma bands of  $^{112}\text{Ru}$ , based on cross-checking using our high statistics data and the less-compressed cube, we disagree on the 918 keV transition feeding the  $12^+$  level reported in Ref. 7 and, instead, in our work an 893.3 keV transition was substituted to de-excite the 4764.1 keV,  $14^+$  level, with a tentative weak 936.5 keV feeding the  $14^+$  level from the  $16^+$  level. Wu *et al.*<sup>7</sup> have only observed the lowest 224 keV  $\Delta I = -1$  linking transition, and have not indicated on their level scheme (their Fig. 7) for  $^{112}\text{Ru}$  the other four weaker cascade transitions ( $\Delta I = -1$ ) coming down from the  $7^+$  level (Fig. 4). Also their level scheme (Fig. 7 in Ref. 7) shows only five transitions de-exciting the one-phonon quasi-gamma band to the ground band. Our level scheme shows eight such transitions out of this band. In addition, as mentioned above, the weakly populated two-phonon quasi-gamma band (3) was identified in  $^{110}\text{Ru}$  and  $^{112}\text{Ru}$  in our work, but not reported in Refs. 6 and 7.

Our energy levels of the ground band (1) in  $^{110}\text{Ru}$  extend to 6050.8 keV,  $18^+$ , while in Wu *et al.*<sup>7</sup> their band goes up to a 8161.1 keV,  $22^+$  level. The weaker band (8) observed in our work is not reported by Wu *et al.*<sup>7</sup> They have not indicated on their level scheme (their Fig. 6) for  $^{110}\text{Ru}$  our four weaker cascade transitions ( $\Delta I = -1$ ) below the  $6^+$  level. Also they have not indicated a doubling above the  $8^+$  level at 2397.0 keV in the one-phonon quasi-gamma band (Fig. 3). We find those two (presumed from their energies) E2 crossover transitions of 843.9 keV and 716.0 keV to be stronger and corresponding to lower excitations than the other sequence (899.6–857.3 keV cascade) above  $8^+$ . Also their level scheme shows only three transitions carrying the one-phonon quasi-gamma band down to the ground band. Our level scheme shows nine such transitions out of the quasi-gamma band.

For band (8) in  $^{110}\text{Ru}$ , which could be some kind of doubling partner of the ground band, we have indicated tentative spin/parity assignments in parentheses. We observed six transitions from band (8) decaying to the ground band and one-phonon quasi-gamma band. If band (8) is even-parity, we expect only E2 or M1 transitions or mixtures of these multipolarities. The lowest observed level at 3193.3 keV is well anchored in energy by its three de-exciting transitions. Its tentative spin of 10 is assigned by virtue of its decay only to spin 8 and 9 levels and not to spin 7 or lower. The next level up in band (8) has its energy anchored by three

de-exciting transitions. The fact that all three final states are spin 10, strongly argues for these being stretched E2 transitions from a spin 12 level. The level at 4370.5 keV has its energy anchored by two de-exciting transitions, both to spin 12, suggesting a  $14^+$  assignment. The next two higher levels have only one de-exciting transition, but their energies are the logical extension by the rotational energy formula that goes as the square of the spin.

We cannot rule out that the 3193.3 keV bandhead is spin/parity  $9^-$ , and the progression of energy levels up this band could have odd-parity assignments with odd spins one unit less than our tentative spin assignments in the level scheme of Fig. 3. In this case, all six decay-out transitions from band (8) would be electric dipole E1. We can probably rule out bandhead spin/parity of  $9^+$  because there should then have been E2 transitions out to  $7^+$ ,  $9^+$ , and  $11^+$ . The stray level at 3193.3 keV could be either  $10^+$  or  $9^-$  on the basis of the above arguments. It would be of much interest to have measurements of the  $\gamma$ - $\gamma$  or fission-fragment- $\gamma$  angular correlations of one or more of the decay-out transitions from band (8) to determine if they are quadrupole or dipole or a mixture. However, our data set had insufficient statistics to measure gamma-gamma angular correlations involving levels of band (8).

The low-spin levels not assigned to a numbered band are mostly levels seen earlier in beta-decay studies of their Tc beta-decay parents. Beta decay of fission products do not heavily contribute to our data, since we only recorded data events with three-fold or higher-fold coincidences. However, where beta-decay results in triple- or higher-fold cascades, we may have a high statistics source of additional data. It is difficult to determine how much of the population of observed levels comes from prompt gammas and how much from beta-delayed gammas. We have included these levels in our  $^{108,110}\text{Ru}$  level schemes and the tables without implication of how much population comes from prompt or delayed. In the case of  $^{108}\text{Ru}$ , the top two members of the  $0^+$  band at 975.9 keV were not reported in beta-decay work and indicate feeding from prompt-fission gammas.

### 3. Discussion

In earlier reports,<sup>2-7</sup> triaxial deformation was proposed in neutron-rich Ru nuclei. In order to understand the structural characteristics of the high-spin states observed in  $^{108,110,112}\text{Ru}$ , we carried out CSM calculations, as described in detail by Bengtsson and Frauendorf.<sup>25-27</sup> See also the earlier work of Skalski, Mizutori, and Nazarewicz,<sup>28</sup> also Troitenier *et al.*<sup>29</sup> and Chasman.<sup>30</sup> The calculated results in this work are expressed as TRS and Routhians. Calculated TRS plots for  $^{108,110,112}\text{Ru}$  are shown in Fig. 5. It shows that the minima of the TRS are around deformation parameters given in Table 1.

At higher spin, ( $\hbar\omega = 0.4$  MeV) the  $^{108,110,112}\text{Ru}$  nuclei indeed all show triaxial minima. However, the calculated results indicate that in the uncranked ground state, while both the  $^{108,110}\text{Ru}$  nuclei favor triaxial deformation, the  $^{112}\text{Ru}$  nucleus

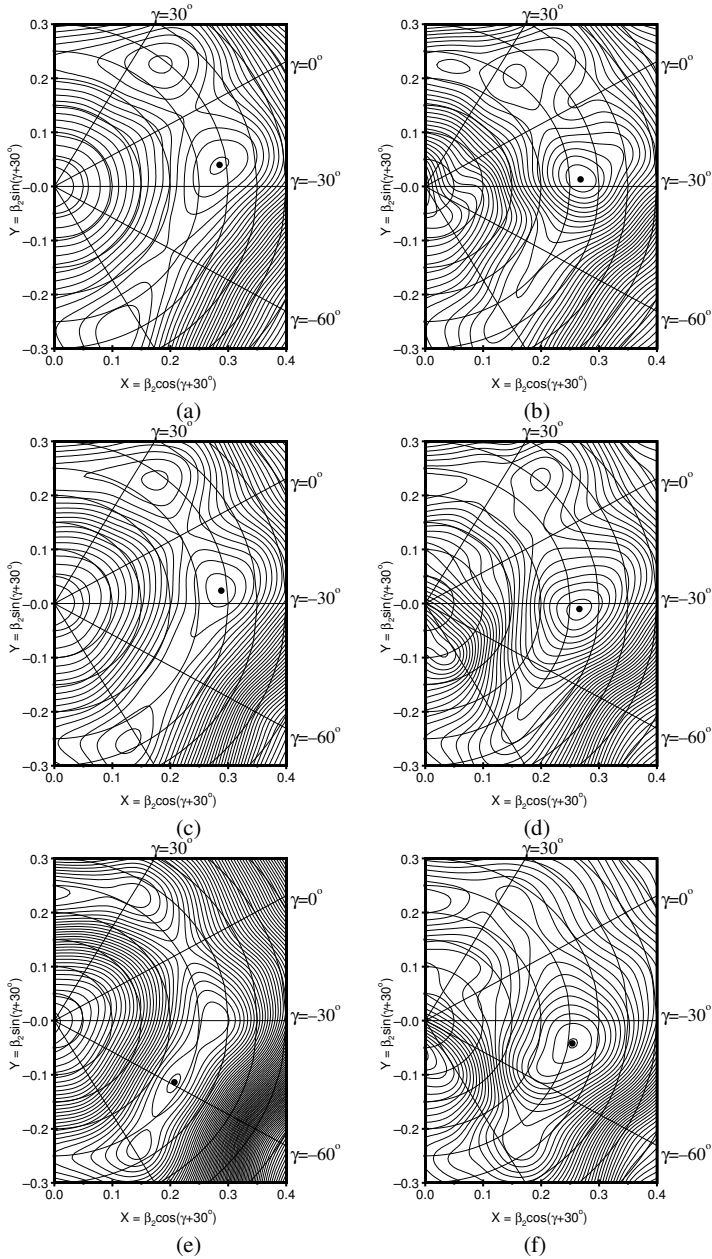


Fig. 5. Polar-coordinate plots of total Routhian surface (TRS) calculated at  $\hbar\omega = 0.0$  and  $0.4$  MeV for  $^{108,110,112}\text{Ru}$ . The leftmost three plots are for zero cranking ( $\hbar\omega = 0.0$ ) and the rightmost three are for cranking velocity of ( $\hbar\omega = 0.4$  MeV). The top two plots are for  $^{108}\text{Ru}$ ; the middle two for  $^{110}\text{Ru}$ , and the lowest two for  $^{112}\text{Ru}$ . Note that the deepest minima in uncranked and cranked examples are near the maximum triaxiality except for uncranked  $^{112}\text{Ru}$ , where the deepest minimum is for an oblate shape, with a secondary minimum near pure triaxiality.

Table 1. Deformation parameters of the TRS minima for  $\hbar\omega = 0.0$  and  $\hbar\omega = 0.4$  MeV for  $^{108,110,112}\text{Ru}$ .

Nucleus	$\hbar\omega$ (MeV)	$\beta_2$	$\beta_4$	$\gamma$ ( $^\circ$ )
$^{108}\text{Ru}$	0.0	0.29	0.004	-22
	0.4	0.27	-0.010	-27
$^{110}\text{Ru}$	0.0	0.29	-0.005	-25
	0.4	0.27	-0.02	-32
$^{112}\text{Ru}$	0.0	0.24	-0.05	-59
	0.4	0.26	-0.026	-39

favors oblate deformation. The ground state (low-spin) TRS energy surfaces may be qualitatively compared with the HF energy surfaces shown in Fig. 8 of Äystö *et al.*<sup>2</sup> In the HF surfaces of the same three nuclei, there is never an oblate minimum. There is a single minimum around  $15^\circ$  for 108 and 110, and a double minimum at prolate and triaxial with a low saddle between minima for 112. We note that Wu *et al.*<sup>7</sup> also present CSM theoretical calculations of  $^{112}\text{Ru}$  for triaxial shapes on both prolate ( $\gamma = -26^\circ$ ) and oblate sides ( $\gamma = -34^\circ$ ) of maximum triaxiality both for quasi-protons and quasi-neutrons. In our TRS calculations of the shape-energy surface (Fig. 5), we see near maximum triaxiality minima in all three ruthenium isotopes, with a tendency to shift from prolate side toward oblate side with increasing mass number. With no cranking our  $^{112}\text{Ru}$  surface shows two minima, the deeper one at oblate spheroidal, and a secondary minimum near maximum triaxiality. (See also Bengtsson *et al.*<sup>31</sup> for the energy surface for  $^{108}\text{Ru}$ , showing a minimum of  $\epsilon_2$  of 0.28 and  $\gamma$  of  $22^\circ$ , similar to that in our Fig. 5(a).)

We believe that these shape/energy surfaces in this region of nuclei may depend sensitively on the choice of spherical single-particle orbital energies. This region has the Fermi energy near both downgoing (prolate-driving) and upgoing (prolate-weakening) Nilsson orbitals, so that there is a balance in determination of shape minima and valleys. It should, thus, not be surprising that there are some differences among the different theoretical shape calculations.

The plots of the kinetic moment-of-inertia  $J^{(1)}$  as a function of rotational frequency  $\hbar\omega$  for the ground bands of  $^{108,110,112}\text{Ru}$  are shown in Fig. 6, along with that of the side band (8) in  $^{110}\text{Ru}$ . It shows that the band-crossing of the ground band in  $^{108,110,112}\text{Ru}$  occur at a rotational frequency  $\hbar\omega \sim 0.40$  MeV, but the  $^{108}\text{Ru}$  and  $^{110}\text{Ru}$  show a sharp crossing while the  $^{112}\text{Ru}$  shows a soft crossing (upbending). We also carried out calculations of Routhians for  $^{108,110,112}\text{Ru}$  using CSM. As an example, calculated Routhians for  $^{108}\text{Ru}$  are presented in Fig. 7(a) for protons and Fig. 7(b) for neutrons, respectively. The calculations predict that a band-crossing caused by the alignment of two  $h_{11/2}$  neutrons occurs at  $\hbar\omega \sim 0.4$  MeV, which well agrees with the experimental value of  $\hbar\omega \sim 0.40$  MeV, whereas the band-crossing related to the alignment of two  $g_{9/2}$  protons cannot be seen in the calculations, which

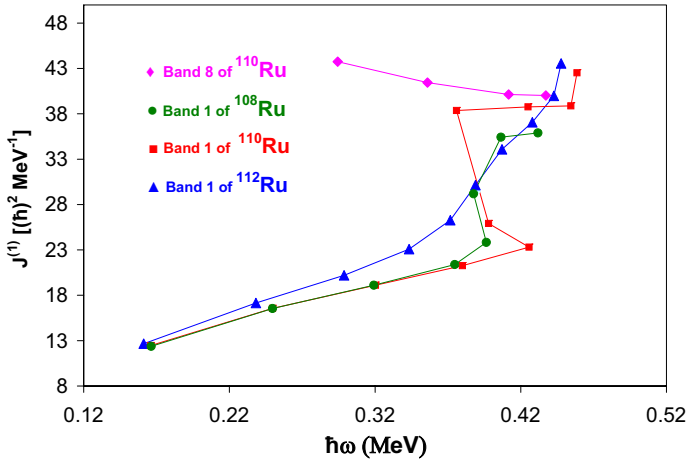


Fig. 6. (color online) Kinetic moments-of-inertia for the ground band (1) in  $^{108,110,112}\text{Ru}$  and band (8) in  $^{110}\text{Ru}$ . There is sharp band-crossing for  $^{108,110}\text{Ru}$  and soft upbending for  $^{112}\text{Ru}$ , all associated with alignment of a pair of  $h_{11/2}$  neutrons. The curious band in  $^{110}\text{Ru}$  is also plotted.

go up to 0.6 MeV. The calculated Routhians in  $^{110,112}\text{Ru}$  show similar behavior. Thus, we believe that  $h_{11/2}$  neutron pair alignment is responsible for the sharp band-crossing in the ground band in  $^{108,110}\text{Ru}$  and upbending (soft band-crossing) in the ground band in  $^{112}\text{Ru}$ .

The  $J^{(1)}$  plots of the one-phonon quasi-gamma bands of  $^{108,110,112}\text{Ru}$  are shown in Figs. 8(a), (b) and (c), respectively. Here we label the bands with the total signature  $\alpha_t$ , as defined by Bengtsson and Frauendorf<sup>32</sup> and reiterated in the Table of Isotopes.<sup>33</sup> The alternative label  $r_t$  was defined as equal to  $e^{-i\pi\alpha_t}$ . It can be seen in the figure that  $J^{(1)}$  of  $^{112}\text{Ru}$  varies smoothly with increasing rotational frequencies in the rotational frequency region for both members of the band (Fig. 8(c)). For  $^{108}\text{Ru}$ , however, while the  $\alpha_t = 0$  ( $r = +1$ ) even-spin branch varies smoothly with rotational frequencies the  $\alpha_t = \pm 1$  ( $r = -1$ ) odd-spin branch of the band shows a band-crossing at  $\hbar\omega \sim 0.35$  MeV (Fig. 8(a)). It is of interest to note that the doubling of the  $\alpha_t = 0$  ( $r = +1$ ) even-spin branch at  $8^+$  in  $^{110}\text{Ru}$  (see Fig. 8(b)) results in two sub-branches and one of them exhibits band-crossing at  $\hbar\omega \sim 0.35$  MeV.

The states of the one-phonon quasi-gamma bands (2) in  $^{108,110,112}\text{Ru}$  contain substantial admixtures of even-numbered  $K$  values less than or equal to the spin. This admixing is a consequence of the triaxial shape or softness, evidenced by the relatively low-lying  $2^+$  bandheads at 707.9 keV in  $^{108}\text{Ru}$ , 612.7 keV in  $^{110}\text{Ru}$  and 523.6 keV in  $^{112}\text{Ru}$ . Figure 9 shows the signature splitting of the quasi-gamma band in the three adjacent even-even ruthenium isotopes, using the splitting expression  $S(I)$  used by the Cologne group (cf. Gelberg *et al.*<sup>34</sup>) which for the case of degenerate levels shows an absolute value of  $|1|$ . The isotope  $^{108}\text{Ru}$  shows a signature-splitting pattern that is fairly constant with increasing spin. For  $^{110}\text{Ru}$

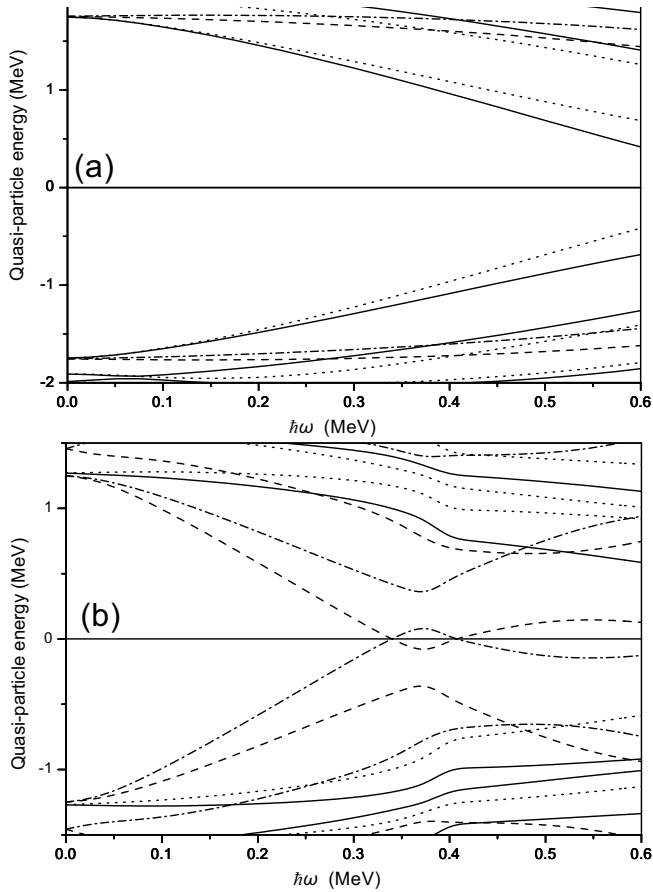


Fig. 7. Calculated Routhians in  $^{108}\text{Ru}$  for both quasi-protons (a) and quasi-neutrons (b) are plotted against rotational frequency. The parity and signature  $(\pi, \alpha)$  of the levels are:  $-(+, +)$ ;  $\cdots (+, -)$ ;  $-\cdot-\cdot (-, +)$ ;  $--- (-, -)$ . No band-crossing is seen for protons out to the 0.6 MeV plotted. A neutron band-crossing is predicted slightly below  $\hbar\omega \sim 0.4$  MeV.

the signature splitting starts with the same sign as  $^{108}\text{Ru}$  at the low end of the band, then is almost flat and finally changes to the opposite sign from that in  $^{108}\text{Ru}$ . The signature splitting in  $^{112}\text{Ru}$  starts small with opposite sign from the other two isotopes and steadily increases with the same sign until it has the largest signature splitting among the three isotopes. For large spins it has the same sign as  $^{110}\text{Ru}$  and opposite sign from  $^{108}\text{Ru}$ . There are many publications dealing with signature splitting in gamma and quasi-gamma bands.

Table 2 shows our measured excitation energies and energy ratios between the two-phonon quasi-gamma bandhead,  $4^+$ , and the one-phonon quasi-gamma bandhead,  $2^+$ , in  $^{108,110,112}\text{Ru}$  and those in  $^{104,106}\text{Mo}$ . One can see that the values for  $^{104,106}\text{Mo}$  are near 2, whereas the values for  $^{108,110,112}\text{Ru}$  are progressively larger

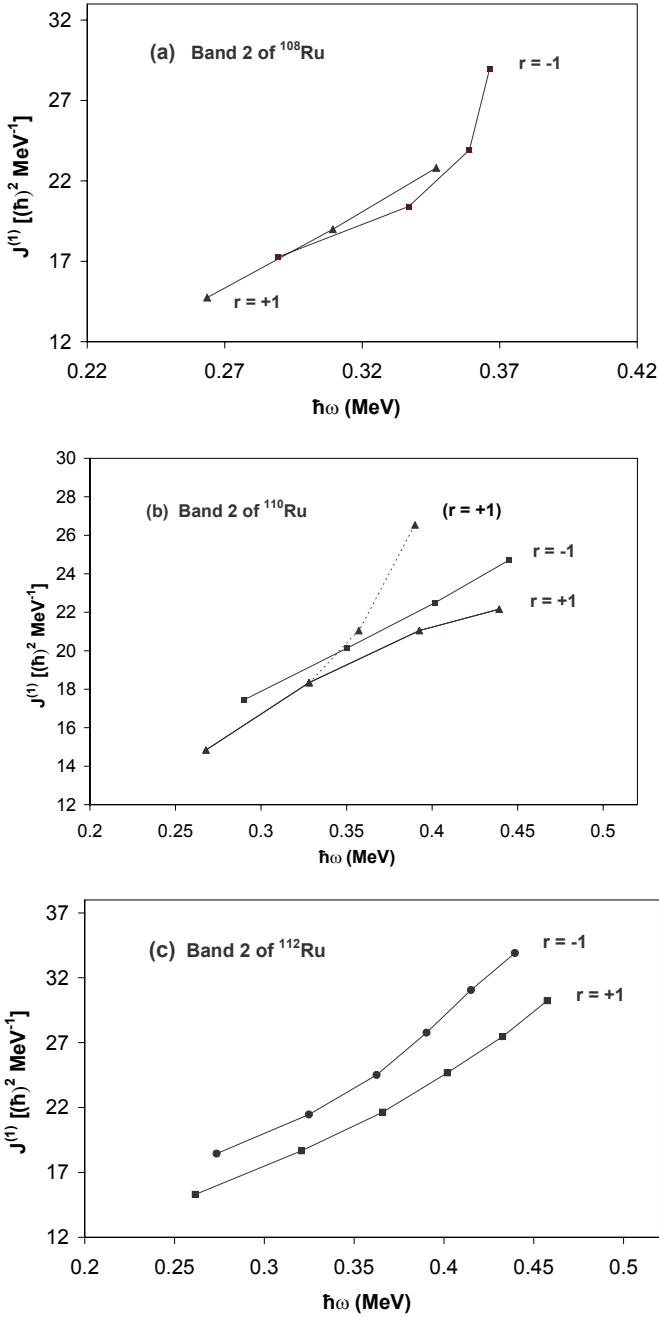


Fig. 8. Kinetic moments-of-inertia for the one-phonon quasi-gamma bands (2) in  $^{108,110,112}\text{Ru}$ , respectively. Note the up-banding of the branch after the doubling at  $8^+$  of the one-phonon quasi-gamma bands (2) in  $^{110}\text{Ru}$ . Even spins are in bands labeled by signature  $r = +1$  and odd spins by  $r = -1$ .

than 2. The larger ratio value surely indicates that there is increasing anharmonicity with increasing neutron number. The  $B(E2)$  branching ratios from the bandhead ( $4^+$ ) of the two-phonon quasi-gamma band (band 3) feeding the  $2^+$  of the ground band and the excited  $2^+$  of the one-phonon quasi-gamma (band 2) are measured to be 0.09 for  $^{108}\text{Ru}$  and 0.03 for  $^{110}\text{Ru}$ . The ratio is too small to be measured for  $^{112}\text{Ru}$ . The  $B(E2)$  ratios show strong preference for decay to the one-phonon quasi-gamma band instead of the ground band, and these phonon-number selection rules get progressively stronger in going from  $^{108}\text{Ru}$  to  $^{110}\text{Ru}$  to  $^{112}\text{Ru}$ . The weaker selection rule in  $^{108}\text{Ru}$  can be attributed to more admixture of configurations other than the dominant two-phonon component. Indeed, in the level scheme of  $^{108}\text{Ru}$ , the proposed 1643.9 keV,  $4^+$ , two-phonon quasi-gamma bandhead is only 5 keV above the 1638.8 keV,  $4^+$  level of the excited  $0^+$  band. Though the mixing matrix element is small, the weak branching into the 1249.2 keV  $2^+$  level of the excited  $0^+$  band provides additional evidence for the mixing (see Fig. 2 and Table 3). The strong decay-out of the ( $4^+$ ) state of band 3 feeding the one-phonon quasi-gamma band thus provides further evidence for the interpretation of band 3 as a two-phonon quasi-gamma band in  $^{110,112}\text{Ru}$ , and the 1643.9 keV level as the bandhead of  $^{108}\text{Ru}$ .

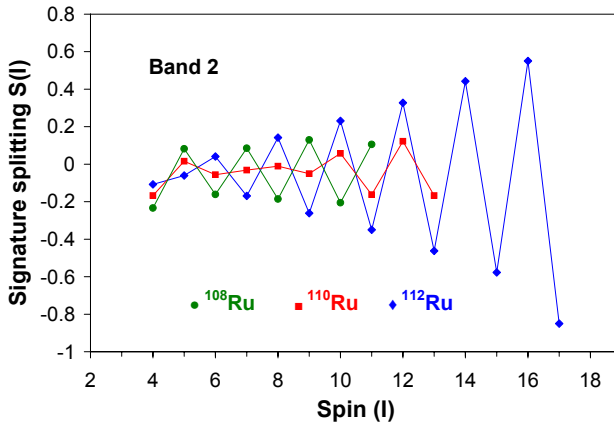


Fig. 9. (color online) Signature splittings of the one-phonon quasi-gamma band (2) in  $^{108,110,112}\text{Ru}$ . See discussions in the text.

Table 2. Energies (keV) and ratios of one- and two-phonon quasi-gamma bandheads.

	$^{104}\text{Mo}$	$^{106}\text{Mo}$	$^{108}\text{Ru}$	$^{110}\text{Ru}$	$^{112}\text{Ru}$
$E_{4^+_3}$	1583.4	1434.9	1643.9	1618.4	1413.9
$E_{2^+_2}$	812.0	710.6	707.9	612.7	523.6
$E_{4^+_3}/E_{2^+_2}$	1.95	2.02	2.32	2.64	2.70

We also point out that Shannon *et al.*<sup>3</sup> early dealt in detail with branching ratios in Mo and Ru even–even gamma bands and made comparisons with the Rigid Triaxial Rotor model predictions. Our Tables 3–5 list the energy and branching-decay transition relative intensities of levels in 108, 110, and 112 ruthenium isotopes, respectively. For comparison we list our measured branching ratios (in parentheses) with their statistical standard deviations following in italics, and current (March 2007) ENSDF Brookhaven evaluated database values [in square brackets] where available. The most intense of the branching decay-out transition for each level is taken as relative intensity 100. We have omitted the Shannon *et al.*<sup>3</sup> branching

Table 3.  $^{108}\text{Ru}$  levels and their gamma-ray branching relative intensities.

$^{108}\text{Ru}$ levels (keV)	Spin/parity	Decaying transitions $E_\gamma$ (keV)		Band
		(our branching)	and [ENSDF branching]	
242.3	$2^+$	242.3 (100)	[100]	1
665.2	$4^+$	422.9 (100)	[100]	1
1240.8	$6^+$	574.8 (100)	[100]	1
1941.7	$8^+$	701.7 (100)	[100]	1
2739.3	$10^+$	797.6 (100)	[100]	1
3527.7	$12^+$	788.4 (100)	[100]	1
4289.9	$14^+$	762.2 (100)	[100]	1
5153.3	$16^+$	863.4 (100)	[100]	1
707.9	$2^+_{2}$	465.6 (100)	[100]; 707.8 (89.0 <i>2.4</i> ) [80 9]	2
974.9	$3^+$	732.6 (100)	[100]; 267.1 (9.4 <i>0.5</i> ) [10.8 <i>1.9</i> ]; 309.6 (4.3 <i>0.5</i> ) [6.3 <i>0.9</i> ]	2
1182.9	$4^+_{2}$	475.0 (100)	[100]; 517.6 (71.3 <i>2.6</i> ) [63 <i>22</i> ]; 940.8 (36.3 <i>1.8</i> ) [23 <i>11</i> ]; 207.9 (3.4 <i>0.6</i> )	2
1495.9	$5^+$	521.0 (100)	[100]; 830.6 (58.4 <i>2.7</i> ) [50]; 312.9 (10.0 <i>2.2</i> )	2
1762.3	$6^+_{2}$	579.4 (100)	[100]; 1097.1 (13.7 <i>0.6</i> ); 522.4 (13.6 <i>1.1</i> ) [17]	2
2132.8	$7^+$	636.9 (100);	892.9 (29.0 <i>2.5</i> )	2
2419.9	$8^+_{2}$	657.6 (100)	[100]	2
2843.3	$9^+$	710.5 (100);	901.8 (5.4 <i>1.0</i> )	2
3149.7	$10^+_{2}$	729.8 (100)		2
3568.8	$11^+$	725.5 (100);	829.6 (5.1 <i>1.1</i> )	2
4308.4	$13^+$	739.6 (100)		2
1643.9	$(4^+)_4$	668.9 (100)	[100]; 936.0 (78.3 <i>4.7</i> ) [41 <i>11</i> ]; 1401.5 (52.2 <i>3.1</i> ) [73 <i>16</i> ]; 394.6 (43.5 <i>2.6</i> ) [36 <i>11</i> ]	
1825.9	$2^+_{5}$	1583.4 (100)	[100]; 1118.0 (83 <i>4</i> ) [48 <i>7</i> ]; 850.9 (67 <i>4</i> ) [33 <i>4</i> ]; 576.5 (17 <i>1</i> ) [18 <i>4</i> ]; 182.0 (17 <i>2</i> ) [9.2 <i>1.9</i> ]	
975.9	$0^+_{2}$	733.6 (100)	[100]	
1249.2	$2^+_{3}$	1007.1 (100)	[100]; 1249.1 (81.3 <i>4.1</i> ) [67 <i>15</i> ]; 584.0 (overlapped) [28 <i>10</i> ]; 273.4 (25.0 <i>1.5</i> ) [11 <i>3</i> ]; 541.3 (25.0 <i>2.1</i> ) [14.8 <i>2.9</i> ]	
1638.8	$(4^+)_3$	389.6 (100)		
2091.1	$(6^+)_3$	452.3 (100)		

Table 4.  $^{110}\text{Ru}$  levels and their gamma-ray branching relative intensities.

$^{110}\text{Ru}$ levels (keV)	Spin/parity	Decaying transitions $E_\gamma$ (keV)		Band
		(our branching) and [ENSDF branching]		
240.8	$2^+$	240.8 (100)	[100]	1
663.5	$4^+$	422.6 (100)	[100]	1
1239.2	$6^+$	575.7 (100)	[100]	1
1944.5	$8^+$	705.3 (100)	[100]	1
2759.5	$10^+$	815.0 (100)	[100]	1
3647.1	$12^+$	887.6 (100)	[100]	1
4351.0	$14^+$	703.9 (100); 650.9 (14.0 0.4)		1
5150.7	$16_2^+$	799.7 (100)		1
6050.8	$18_2^+$	900.1 (100)		1
3700.1	$(12^+)_2$	940.5 (100)		1
612.7	$2_2^+$	371.9 (100) [100]; 612.7 (81.9 1.0) [93 7]		2
859.9	$3^+$	619.1 (100) [100]; 247.3 (20.6 0.3) [22 3]; 196.5 (1.5 0.2)		2
1084.5	$4_2^+$	471.7 (100) [100]; 421.0 (50.6 1.5) [49 9]; 843.6 (15.9 1.0) [17 5]; 224.5 (2.7 0.2)		2
1375.4	$5^+$	515.5 (100) [100]; 711.9 (20.3 0.6) [17 4]; 291.0 (3.6 0.2)		2
1684.3	$6_2^+$	599.8 (100) [100]; 1021.0 (23.0 3.5) [30 16]; 445.2 (11.1 0.7) [9.4 2.7]; 308.7 (7.7 0.4);		2
2021.0	$7^+$	645.5 (100) [100]; 781.7 (7.4 0.7)		2
2397.0	$8_2^+$	712.7 (100) [100]; 452.5 (12.9 1.9)		2
2777.0	$9^+$	756.0 (100)		2
3254.3	$10_4^+$	857.3 (100)		2
3627.1	$11^+$	850.2 (100)		2
4153.9	$12_5^+$	899.6 (100)		2
4556.1	$13^+$	929.0 (100)		2
3113.0	$(10^+)_2$	716.0 (100)		2
3956.9	$(12^+)_4$	843.9 (100)		2
1618.4	$(4^+)_3$	1005.7 (100); 758.5 (66.7 4.4); 534.0 (26.7 2.1); 1377.6 (13.3 0.8)		3
1860.8	$(5^+)_2$	242.4 (100); 776.4 (12.5 0.8); 1000.9 (12.5 1.1)		3
2110.8	$(6^+)_3$	1026.4 (100); 492.4 (42.9 4.7); 735.4 (4.8 0.6)		3
3193.3	$(10^+)_3$	416.4 (100); 1249.0 (51.0 4.7); 796.3 (23.9 5.0)		8
3719.0	$(12^+)_3$	525.7 (100); 959.5 (7.1 1.2); 464.9 ( $\leq 2.9$ )		8
4370.5	$(14^+)_2$	651.5 (100); 670.4 ( $\leq 1.8$ )		8
5143.0	$(16^+)_1$	772.5 (100)		8
6017.4	$(18^+)_1$	874.4 (100)		8
1656.1	$2_4^+$	796.3 (100) [ $\leq 56$ ]; 1415.4 (87.5 4.4) [100 20]; 1043.6 (25.0 2.0)		

Table 4. (Continued)

$^{110}\text{Ru}$ levels (keV)	Spin/parity	Decaying transitions $E_\gamma$ (keV) (our branching) and [ENSDF branching]	Band
1820.5	$(2_5^+, 3_2^+)$	423.5 (100) [100]; 164.5 (31 2) [38 7]; 1579.8 (25.0 2.1) [48 12]; 960.5 (25.0 2.5) [32 12]	
2042.4		221.9 (100)	
1137.3	$(0^+)_2$	896.4 (100)	
1396.9	$2_3^+$	1156.2 (100) [100]; 1396.9 (44.4 2.9) [50 20]; 537.2 (33.3 2.7); 783.9 (22.2 1.6); 733.3 (22.2 2.7); 259.6	

ratios from the tables, since no standard deviations were given. However, we do show as (100)[100] those levels observed by us and also recorded in ENSDF. The ENSDF includes fission-gamma work up to Shannon *et al.*<sup>3</sup> but not later work.

The measurements of the gamma branching ratios from various levels usually involved double-gating on cascade transitions from above the level of interest and least squares peak-fitting of all branching transitions using the gf3 program in the Radware package. The relative peak areas and their statistical standard deviations were divided by the relative gamma-detection efficiency for each transition energy. The strongest branch intensity was set as reference of 100. The percentage standard deviations of branches relative to the reference were taken as the square root of the sum of the squares of the percentage deviations of the given transition to the reference transition. This method of determining branching ratios eliminates some of the sources of systematic deviations, such as, the detection efficiencies of the gating transitions. The result depends not on the absolute detection efficiencies at the energy of each branching transition but only on the relative efficiencies of the branch and the reference transition. We are not able to estimate systematic errors, such as those arising from energy dependence of efficiency curves, so our statistical standard deviations may seem small, especially compared to the ENSDF values taken mainly from beta-decay studies. The data evaluators for ENSDF may use judgment in taking weighted averages of relative intensities reported by independent investigations, giving larger posted standard deviations. We believe that the high statistics of our data lend themselves to the better branching ratio numbers.

A clear feature observed in one-phonon quasi-gamma bands of the Ru isotopes is that all the quasi-gamma bandhead-to-ground transition matrix elements  $B(E2)$  are weak, relative to the  $2^+$  bandhead to  $2^+$  ground transition by Alaga rules for good  $K$  quantum numbers. The transition to ground vanishes at maximum triaxiality of  $\pm 30^\circ$  if the irrotational-flow moment-of-inertia ratios among the three principal axes holds, as shown in Eq. (36) of Ref. 34. The  $\Delta I = 0$  transitions from higher spins ( $4^+, 6^+, \dots$ ) also predominate over the  $\Delta I = -2$  transitions, as seen in branching ratio Tables 3–5.

The observation of the possible doubling band (8) in  $^{110}\text{Ru}$  is a challenge to theory. It is interesting that, unlike  $^{110}\text{Ru}$ , no similar nearly degenerate sideband to the ground band is yet found in  $^{108,112}\text{Ru}$ . The strongest branching out of the band

Table 5.  $^{112}\text{Ru}$  levels and their gamma-ray branching relative intensities.

$^{110}\text{Ru}$ levels (keV)	Spin/parity	Decaying transitions $E_\gamma$ (keV) (our branching) and [ENSDF branching]	Band
236.8	$2^+$	236.8 (100) [100]	1
645.0	$4^+$	408.2 (100) [100]	1
1189.7	$6^+$	544.7 (100) [100]	1
1839.7	$8^+$	650.0 (100) [100]	1
2562.7	$10^+$	723.0 (100) [100]	1
3325.9	$12^+$	763.2 (100)	1
4118.1	$14^+$	792.2 (100)	1
4954.3	$16^+$	836.2 (100)	1
5829.7	$18^+$	875.4 (100)	1
6725.1	$20^+$	895.4 (100)	1
523.5	$2^+$	286.8 (100) [100]; 523.6 (91.8 1.4) [82 17]	2
747.6	$3^+$	510.8 (100) [100]; 224.0 (35.1 0.6) [36 8]	2
980.7	$4^+$	457.2 (100) [100]; 335.6 (22.9 1.0) [20 6]; 744.1 (3.6 0.3) [6.9 1.8]; 233.2 (5.6 0.6)	2
1235.3	$5^+$	487.8 (100) [100]; 590.5 (6.9 0.4) [7 2]; 54.7 (5.7 0.2)	2
1570.0	$6^+$	589.3 (100) [100]; 334.8 (2.6 0.3); 380.3(1.2 0.2) [15 9]	2
1841.0	$7^+$	605.7 (100) [100]; 270.8 (4.1 0.5); 651.2	2
2263.3	$8^+$	693.3 (100) [100]	2
2534.6	$9^+$	693.6 (100) [100]	2
3033.5	$(10^+)_2$	770.1 (100)	2
3290.9	$(11^+)$	756.3 (100)	2
3870.8	$(12^+)_2$	837.3 (100)	2
4095.9	$(13^+)$	804.9 (100)	2
4764.1	$(14^+)_2$	893.3 (100)	2
4951.2	$(15^+)$	855.3 (100)	2
5700.7	$(16^+)_2$	(936.6) (100)	2
5854.0	$(17^+)$	902.8 (100)	2
1413.5	$(4^+)_3$	890.0 (100); 666.3 (15.4 0.7)	3
1649.5	$(5^+)_2$	235.9 (100); 902.1 (22.2 1.1); 668.9 (5.6 0.4)	3
1955.6	$(6^+)_3$	542.0 (100); 975.0 (62.5 3.3); 720.5 (12.5 0.7)	3
2231.3	$(7^+)_2$	581.9 (100); 995.8 (68.2 4.1)	3
2574.5	$(8^+)_3$	618.9 (100)	3
2909.2	$(9^+)_2$	677.9 (100)	3
2392.0		1156.6 (100)	
2899.8		1058.8 (100); 507.9	
3519.8		619.9 (100)	
4213.4		693.6 (100)	

(8)  $10^+$  bandhead is to the  $9^+$  level of the quasi-gamma band. It is notable that the weakly populated doubling band (8) behaves in some ways like chiral doublet bands in some other cases. Namely, the energy separation between like-spin members of bands (8) and (1) is 433.8 keV at the  $10^+$  level but rapidly decreases with increasing

spin. The energy separation crosses over to a negative 7.7 keV at the  $16^+$  level, and is negative 33.4 keV at the  $18^+$  level. The observed cross-band transitions only go from band (8) to band (1) and not in the reverse direction despite there being similar transition energies. The crossover of energies in presumed chiral doublets has been observed in a few other cases, such as, in a likely odd-parity chiral doublet pair in  $^{112}\text{Ru}$ , as seen in our companion paper on the odd-parity bands in the three even-even ruthenium nuclei.<sup>22</sup> There, also, the cross-talk between bands is only in one direction.

#### 4. Summary

High-spin states of  $^{108,110,112}\text{Ru}$  were reinvestigated. The even-parity bands were considerably expanded. Our new TRS calculations indicate that  $^{108,110,112}\text{Ru}$  have triaxial deformation. The band-crossings in the ground bands are interpreted by CSM calculations as  $h_{11/2}$  neutron-pair alignments. Further evidence is provided for the two-phonon quasi-gamma bands. There are unusual doublings of the ground and one-phonon quasi-gamma band above the  $8^+$  level, where a neutron-pair alignment band-crossing starts in  $^{110}\text{Ru}$ . This behavior represents a challenge to theory. Likewise, there are curious reversals of sign in signature splitting of the one-phonon quasi-gamma band in going through this series of nuclei.

#### Acknowledgments

The work at Tsinghua University in Beijing is supported by the Chinese National Natural Science Foundation under Grant No. 10775078, 10575057 and the Major State Basic Research Development Program 2007CB815005. The work at Vanderbilt University, Lawrence Berkeley National Laboratory, Lawrence Livermore National Laboratory, and Idaho National Laboratory are supported, respectively, by U.S. Department of Energy under Grant No. DE-FG05-88ER40407 and Contract Nos. DE-AC03-76SF00098, W-7405-ENG48, and DE-AC07-99ID13727. The Joint Institute for Heavy Ion Research is supported by its members, U. of Tennessee, Vanderbilt, and the U.S. DOE. The authors are indebted for the use of  $^{252}\text{Cf}$  to the office of Basic Energy Sciences, U.S. Department of Energy, through the transplutonium element production facilities at the Oak Ridge National Laboratory.

#### References

1. J. H. Hamilton, A. V. Ramayya, S. J. Zhu, G. M. Ter-Akopian, Y. T. Oganessian, J. D. Cole, J. O. Rasmussen and M. A. Stoyer, *Prog. Part. Nucl. Phys.* **35** (1995) 635.
2. J. Aysto, P. P. Jauho, Z. Janas, A. Jokinen, J. M. Parmonen, H. Penttila, P. Taskinen, R. Beraud, R. Duffait, A. Emsallem, J. Meyer, M. Meyer, N. Redon, M. E. Leino, K. Eskola and P. Dendooven, *Nucl. Phys. A* **515** (1990) 365.
3. J. A. Shannon, W. R. Phillips, J. L. Durell, B. J. Varley, W. Urban, C. J. Pearson, I. Ahmad, C. J. Lister, L. R. Morss, K. L. Nash, C. W. Williams, N. Schulz, E. Lubkiewicz and M. Bentaleb, *Phys. Lett. B* **336** (1994) 136.

4. Q. H. Lu, K. Butler-Moore, S. J. Zhu, J. H. Hamilton, A. V. Ramayya, V. E. Oberacker, W. C. Ma, B. R. S. Babu, J. K. Deng, J. Kormicki, J. D. Cole, R. Aryaeinejad, Y. X. Dardenne, M. Drigert, L. K. Paker, J. O. Rasmussen, M. A. Stoyer, S. Y. Chu, K. E. Gregorich, I. Y. Lee, M. F. Mohar, J. M. Nitschke, N. R. Johnson, F. K. McGowan, G. M. Ter-Akopian, Y. T. Oganessian and J. B. Gupta, *Phys. Rev. C* **52** (1995) 1348.
5. I. Deloncle, A. Bauchet, M. G. Porquet, M. Girod, S. Péru, J. P. Delaroche, A. Wilson, B. J. P. Gall, F. Hoellinger, N. Schulz, E. Gueorguieva, A. Minkova, T. Kutsarova, T. Venkova, J. Duprat, H. Sergolle, C. Gautherin, R. Lucas, A. Astier, N. Buform, M. Meyer, S. Perries and N. Redon, *Eur. Phys. J. A-Hadrons Nucl.* **8** (2000) 177.
6. H. Hua, C. Y. Wu, D. Cline, A. B. Hayes, R. Teng, R. M. Clark, P. Fallon, A. Goergen, A. O. Macchiavelli and K. Vetter, *Phys. Lett. B* **562** (2003) 201.
7. C. Y. Wu, H. Hua, D. Cline, A. B. Hayes, R. Teng, D. Riley, R. M. Clark, P. Fallon, A. Goergen, A. O. Macchiavelli and K. Vetter, *Phys. Rev. C* **73** (2006) 34312.
8. P. Möller, R. Bengtsson, B. G. Carlsson, P. Olivius and T. Ichikawa, *Phys. Rev. Lett.* **97** (2006) 162502.
9. M. Sakai, *Nucl. Data, Sect. A* **10** (1972) 201.
10. A. S. Davydov and G. F. Filippov, *Nucl. Phys.* **8** (1958).
11. S. Frauendorf and J. Meng, *Nucl. Phys. A* **617** (1997) 131.
12. V. Dimitrov, S. Frauendorf and F. Dönau, *Phys. Rev. Lett.* **84** (2000) 5732.
13. T. Koike, K. Starosta, C. J. Chiara, D. B. Fossan and D. R. LaFosse, *Phys. Rev. C* **63** (2001) 61304.
14. K. Starosta, T. Koike, C. J. Chiara, D. B. Fossan, D. R. LaFosse, A. A. Hecht, C. W. Beausang, M. A. Caprio, J. R. Cooper, R. Krücken, J. R. Novak, N. V. Zamfir, K. E. Zyranski, D. J. Hartley, D. L. Balabanski, J.-Y. Zhang, S. Frauendorf and V. I. Dimitrov, *Phys. Rev. Lett.* **86** (2001) 971.
15. S. J. Zhu, in *Proc. Third Int. Conf. on Fission and Properties of Neutron-Rich Nuclei, Sanibel Island, Florida*, eds. A. V. Hamilton, J. H. Ramayya and H. K. Carter (World Scientific, Singapore, 2003), pp. 191–198.
16. S. J. Zhu, *The Fourth International Conference on Exotic Nuclei and Atomic Masses* (Springer, Pine Mountain, GA, 2004), pp. 459–462.
17. J. H. Hamilton, S. J. Zhu, Y. X. Luo, A. V. Ramayya, J. O. Rasmussen, S. Frauendorf, J. K. Hwang and J. Y. Zhang, Evidence for and against chiral bands in nuclei, in *Proc. 11th Annual International Conference on Nuclear Reaction Mechanisms*, Varenna, Italy, 2006, ed. E. Gadioli (Archimede snc, Rozzano (Mi), Varenna, Italy, 2007), p. 419.
18. Z. Jiang, S. J. Zhu, J. H. Hamilton, A. V. Ramayya, J. K. Hwang, Z. Zhang, R. Q. Xu, S. D. Xiao, X. L. Che, U. Yong-Nan, W. C. Ma, J. D. Cole, M. W. Drigert, I. Y. Lee, J. O. Rasmussen and Y. X. Luo, *Chin. Phys. Lett.* **20** (2003) 350.
19. X. L. Che, S. J. Zhu, J. H. Hamilton, A. V. Ramayya, J. K. Hwang, J. O. Rasmussen, Y. X. Luo, Y. J. Chen, M. L. Li and H. B. Ding, *Chin. Phys. Lett.* **23** (2006) 328.
20. I. Stefanescu, A. Gelberg, J. Jolie, P. Van Isacker, P. von Brentano, Y. X. Luo, S. J. Zhu, J. O. Rasmussen, J. H. Hamilton, A. V. Ramayya and X. L. Che, *Nucl. Phys. A* **789** (2007) 125.
21. D. C. Radford, *Nucl. Instr. Meth. Phys. Res. A* **361** (1995) 297.
22. Y. X. Luo, S. J. Zhu, J. H. Hamilton, A. V. Ramayya, C. Goodin, K. Li, X. L. Che, J. K. Hwang, I. Y. Lee, G. M. Ter-Akopian, A. V. Daniel, M. A. Stoyer, R. Donangelo, S. Frauendorf, V. Dimitrov, J. Y. Zhang, J. D. Cole, N. J. Stone and J. O. Rasmussen, *Int. Mod. Phys. E* **18** (2009) 1697.

23. X. L. Che, S. J. Zhu, J. H. Hamilton, A. V. Ramayya, J. K. Hwang, U. Yong-Nam, M. L. Li, R. C. Zheng, I. Y. Lee and J. O. Rasmussen, *Chin. Phys. Lett.* **21** (2004) 1904.
24. J. Stachel, N. Kaffrell, N. Trautmann, K. Brodén, G. Skarnemark and D. Eriksen, *Zeitschrift für Physik A Hadrons and Nuclei* **316** (1984) 105.
25. R. Bengtsson, *Nucl. Phys. A* **198** (1972) 591.
26. S. Frauendorf, *Phys. Lett. B* **100** (1981) 219.
27. S. Frauendorf and F. R. May, *Phys. Lett. B* **125** (1983) 245.
28. J. Skalski, S. Mizutori and W. Nazarewicz, *Nucl. Phys. A* **617** (1997) 282.
29. D. Troltenier, J. P. Draayer, B. R. S. Babu, J. H. Hamilton, A. V. Ramayya and V. E. Oberacker, *Nucl. Phys. A* **601** (1996) 56.
30. R. R. Chasman, *Zeitschrift für Physik A Hadrons and Nuclei* **339** (1991) 111.
31. R. Bengtsson, P. Möller, J. R. Nix and J. Zhang, *Phys. Scr.* **29** (1984) 402.
32. R. Bengtsson and S. Frauendorf, *Nucl. Phys. A* **327** (1979) 139.
33. R. B. Firestone and V. S. Shirley (eds.), *Table of Isotopes*, Vol. 2 (John Wiley and Sons, New York, 1996).
34. A. Gelberg, D. Lieberz, P. von Brentano, I. Ragnarsson, P. B. Semmes and I. Wiedenhöver, *Nucl. Phys. A* **557** (1993) 439.

Copyright of International Journal of Modern Physics E: Nuclear Physics is the property of World Scientific Publishing Company and its content may not be copied or emailed to multiple sites or posted to a listserv without the copyright holder's express written permission. However, users may print, download, or email articles for individual use.